
DP-TBART: A Transformer-based Autoregressive Model for Differentially Private Tabular Data Generation

Rodrigo Castellon*
Department of Computer Science
Stanford University
Stanford, CA USA
rjcaste@stanford.edu

Achintya Gopal
Bloomberg
New York, NY USA
agopal6@bloomberg.net

Brian Bloniarz
Bloomberg
San Francisco, CA USA
bbloniarz@bloomberg.net

David Rosenberg
Bloomberg
Toronto, ON Canada
drosenberg44@bloomberg.net

Abstract

The generation of synthetic tabular data that preserves differential privacy is a problem of growing importance. While traditional marginal-based methods have achieved impressive results, recent work has shown that deep learning-based approaches tend to lag behind. In this work, we present Differentially-Private TaBular AutoRegressive Transformer (DP-TBART), a transformer-based autoregressive model that maintains differential privacy and achieves performance competitive with marginal-based methods on a wide variety of datasets, capable of even outperforming state-of-the-art methods in certain settings. We also provide a theoretical framework for understanding the limitations of marginal-based approaches and where deep learning-based approaches stand to contribute most. These results suggest that deep learning-based techniques should be considered as a viable alternative to marginal-based methods in the generation of differentially private synthetic tabular data.

1 Introduction

Though sharing tabular data about individuals can be broadly beneficial (for medical research, for example), privacy concerns typically prevent such data sharing. Differentially private synthetic data generation stands out as an appealing solution to this problem: it provides strong formal privacy guarantees and avoids having to anticipate the exact analysis a downstream analyst might want to conduct, while producing a synthetic dataset that “looks like” the real data from the perspective of an analyst. This problem has received considerable attention from the research community, with a wide variety of approaches available in the literature. Among these, approaches tend to fall into two categories:

- *Marginal-based approaches* make differentially private measurements of low-order marginals, typically represented as histograms, and then fit a generative model to these histograms.

*Work done as an intern at Bloomberg.

- *Deep learning-based approaches* are inspired by successes in domains such as images and text (Li et al., 2021) and train deep neural networks using differentially private optimizers such as DP-SGD (Abadi et al., 2016) to directly fit the data.²

Recent works unambiguously establish marginal-based approaches as state-of-the-art, with performance far surpassing that of approaches using neural networks, which typically fail to adequately model even one-dimensional marginals (Tao et al., 2021; Bowen and Snoke, 2019).

Given the lack of success of deep learning relative to marginal-based approaches, we ask the following question: is this significant gap due to a fundamental inadequacy in the deep learning approach to the task? If not, how can we close this gap?

To answer this question, we present Differentially-Private Tabular AutoRegressive Transformer (DP-TBART), a transformer-based autoregressive model explicitly tailored for the tabular domain, and we show that this simple approach significantly bridges the gap on 10 separate datasets. In addition to narrowing this gap, we provide preliminary results suggesting that this modeling approach serves as a promising direction for downstream use cases that require accurately modeling higher-order interactions among columns.

2 Background & Related Work

2.1 Differential Privacy

Differential privacy (DP), first introduced by Dwork et al. (2006), is a technique used to protect the privacy of individuals in data analysis by preventing attackers from inferring specific information from the data. While many formulations of differential privacy exist, we choose to follow the standard formulation parameterized by ϵ and δ , with lower values providing stronger privacy guarantees. More formally, a differentially-private algorithm is defined as follows:

Definition 2.1. Let $\mathcal{A} : \mathcal{D} \rightarrow \mathcal{S}$ be a randomized algorithm, and let $\epsilon > 0, \delta \in [0, 1]$. We say that \mathcal{A} is (ϵ, δ) -differentially private if for any two neighboring datasets $D, D' \in \mathcal{D}$ differing by a single record, we have that

$$P[\mathcal{A}(D) \in S] \leq e^\epsilon P[\mathcal{A}(D') \in S] + \delta$$

for all $S \subset \mathcal{S}$.

In this paper, we consider a “record” to be a row in a tabular dataset, but this varies depending on the use case. Furthermore, we take “differing by a single record” to mean the addition/removal of an arbitrary record from the dataset (this is known as “unbounded DP”), following the convention set in previous works (Li et al., 2021; McKenna et al., 2022).

More recently, methods for training neural networks in a differentially private manner have been proposed (Abadi et al., 2016; Papernot et al., 2016). In this work, we focus on DP-SGD, a method that preserves privacy throughout training by clipping & perturbing gradients. The per-sample gradients are first projected down to a radius C ball (with C designated as a hyperparameter) in order to bound their sensitivities, and isotropic Gaussian noise is further added to ensure the privacy guarantee is satisfied. The final gradient is obtained by taking the mean of the noised per-sample gradients. Formally, the differentially private estimate of the gradient from a batch of n examples with per-sample gradients g_i is computed as

$$g := \frac{1}{n} \sum_{i=1}^n \left[\min \left(\frac{C}{\|g_i\|}, 1 \right) \cdot g_i + \mathcal{N}(0, C^2 \sigma^2 I) \right]$$

where σ is pre-computed by performing a binary search for the smallest suitable σ that satisfies a desired (ϵ, δ) -DP guarantee for a training run with a set batch size and number of training steps.

²In general, we follow the nomenclature set in Tao et al. (2021). For deep learning-based approaches, we deviate because of the recent development of non-GAN approaches.

2.2 Tabular data generation with deep learning

Many methods for generating tabular data with deep learning have been proposed. Among these, some of the most popular approaches include GANs (Xu et al., 2019; Zhao et al., 2021; 2022) and, more recently, autoregressive models (Borisov et al., 2022; Canale et al., 2022), diffusion models (Kotelnikov et al., 2022), normalizing flows (Lee et al., 2022), VAEs (Xu et al., 2019), and MMD (Harder et al., 2021; Yang et al., 2023).

Unfortunately, while some of these works train with differential privacy, they often neglect to mention the state-of-the-art marginal-based approaches, giving the false impression that these deep learning approaches are state-of-the-art on the task. In contrast, our paper explicitly compares these two approaches on a wide variety of datasets, shows that a performance gap between more recent deep learning methods and marginal-based methods still exists, and demonstrates that autoregressive models can bridge the gap.

Among the methods listed above, (Canale et al., 2022) is the most similar to our method, which presents a universal attention-based modeling strategy for generating synthetic hierarchical data. However, despite the importance of differentially private tabular data generation, the paper presents only a single experiment that validates that their model can achieve competitive performance on this task on a single metric. We expand on these preliminary results and demonstrate that a similar approach is applicable to a wider variety of datasets, and in some limited cases even outperforms state-of-the-art marginal-based methods. Furthermore, we bolster our results with a theoretical framework that sheds light into the specific limitations of marginal-based methods, and *why* deep learning-based methods can sometimes outperform them. As such, this paper stands to be the first to provide a comprehensive comparison between deep learning-based methods and marginal-based methods on the task of differentially private tabular data generation.

2.3 Tabular data generation with marginal-based approaches

In general, marginal-based approaches make differentially-private measurements (e.g., column histograms) and then fit these measurements with a model; both steps may each be performed exactly once (McKenna et al., 2019) or, more often, interleaved many times (Zhang et al., 2017; Liu et al., 2021; McKenna et al., 2022).

Methods that fall under this approach distinguish themselves by (1) which measurements they make and (2) the model used. For example, McKenna et al. (2019) proposes using probabilistic graphical models (PGMs) to represent the distribution. Other methods use Bayesian networks (Zhang et al., 2017) or neural networks (Liu et al., 2021).

The inherent weakness of these methods is that they access all information about the data distribution in the form of low-order marginals, due to the computational complexity of the exponential scaling to high-order marginals. This limitation forces marginal-based methods to prioritize simple correlations at the expense of more complex interactions among columns. We make this intuition more concrete in Section 4.4.1.

3 Method

3.1 Preprocessing

Consistent pre-processing and assumptions about what is considered public or private information is crucial for fair comparisons between methods. In this work, we include datasets with both numeric and categorical column types, and consider the column type (categorical or numerical) as well as their “min” and “max” values to be public (in other words, no DP budget needs to be used to compute max and min).

For the methods “AIM” (McKenna et al., 2022) and “DP-TBART”, we uniformly discretize the numeric columns into 100 bins using the publicly available min and max values. Then, at inference time we invert the discrete values to the midpoint of their original bin edges, rounding to integer values if necessary. For the method “DPCTGAN” (Rosenblatt et al., 2020), values are normalized based on the original min and max.

3.2 Autoregressive Modeling

We adopt a language modeling procedure (akin to many natural language modeling procedures (Vaswani et al., 2017; Radford et al., 2019)) specifically tailored for the discrete tabular setting. Let K be the number of columns in the given dataset. We factorize the probability distribution over a row $X = (X_1, X_2, \dots, X_K)$ with the chain rule:

$$P(X) = P(X_1) \prod_{k=2}^K P(X_k | X_{<k})$$

Note that here, values in each column encode to tokens in a shared vocabulary V while ensuring that no two columns share an encoded value.³ As a consequence, we have that $|V| = \sum_i |V_i|$, where V_i represents the token encodings for column i . The model is defined as a function f_θ that takes a sequence in V^k (with $0 \leq k < K$) and outputs a vector of logits in $\mathbb{R}^{|V|}$. To force the model f_θ to represent a probability distribution over only valid tokens $P(X)$ and thus to output only valid samples, we post-process the model output at each column i and mask out all elements irrelevant to column i . That is, for some sequence x of length k , our revised logit outputs are

$$f'_\theta(x) := f_\theta(x) \odot \mathbf{m}$$

where \odot represents the element-wise (Hadamard) product and \mathbf{m} sets all elements between index $\sum_{i=1}^k |V_i|$ and $\sum_{i=1}^{k+1} |V_i|$ to one and $-\infty$ everywhere else.

We sample from trained models directly, without any further post-processing on the distribution.

3.3 Implementation Details

We adopt a three-layer transformer decoder-only architecture (Vaswani et al., 2017) closely resembling DistilGPT-2 (hidden dimension 768, 12 attention heads) with learned positional encodings and train our models with DP-Adam, learning rate $3e - 4$, and batch size 256 for all of our experiments unless otherwise indicated. During training, we randomly set aside 1% of the data for validation and treat the rest as the training set. For more information, see the Appendix.

4 Experiments

4.1 Experimental Setup

4.1.1 Datasets

We use 10 datasets from various sources for our experiments. Please note that the columns designated as the “Target Variable” are *only* used for evaluation purposes and are not given any special treatment during training. In other words, the fact that a column is a target variable does not influence the training process.

4.1.2 Methods

In addition to DP-TBART, we evaluate the following methods: **AIM** (McKenna et al., 2022), the most recent marginal-based method; **DP-NTK** (Yang et al., 2023), the most recent deep learning-based method; and **DP-MERF** (Harder et al., 2021) and **DP-HFlow** (Lee et al., 2022) and **DPCT-GAN** (Rosenblatt et al., 2020), additional deep learning-based methods.

4.1.3 Evaluation

We evaluate using the following metrics, which are adapted from the Synthetic Data Vault (SDV) (Patki et al., 2016).

³Though we maintain this design choice for all datasets included in Table 2, we share tokens across columns for the Dyck and character-level datasets.

Dataset	# of Rows	Categorical	Numeric	Problem	Target Variable
Adult	48,842	9	5	Classification	income>50K
King	21,613	7	13	Regression	price
Insurance	1,338	4	3	Regression	charges
Loan	5,000	7	7	Classification	Personal Loan
Credit	284,807	1	30	Classification	Class
Bank	45,211	10	7	Classification	y
Census	299,285	35	6	Classification	income
Car	1,728	7	0	Classification	class
Mushroom	8,124	23	0	Classification	poisonous
Poker Hands	25,010	11	0	Classification	10

Table 1: Summary of datasets used in our experiments.

- **Kolmogorov-Smirnov Test (KS):** For numeric columns, this metric computes the Kolmogorov-Smirnov statistic KS (the maximum difference between the CDF of the synthetic and real columns) and returns $1 - KS$. This metric lies between 0 and 1, and higher is better. We average this value across all numeric columns.
- **Chi-Square Test (CS):** For categorical columns, this metric returns the p -value from a chi-square test that checks the null hypothesis that the synthetic data comes from the same distribution as the real data. We average this value across all columns. This metric lies between 0 and 1, and higher is better.
- **Detection (DET):** We train an XGBoost model to differentiate between real and synthetic samples, and then report $1 - ROCAUC$, where $ROCAUC$ is computed as an average of the ROC-AUC scores across several folds. This metric lies between 0 and 1, and higher is better (we would like a classifier to *not* be able to distinguish synthetic data from real data).
- **ML Efficacy (Regression):** We fit a linear regression model to predict a target variable in the dataset on synthetic data and evaluate its performance on the real dataset. This metric returns the r^2 test score. This metric lies below 1, and higher is better.
- **ML Efficacy (Classification):** We fit a decision tree to predict a target variable in the dataset on synthetic data and evaluate its performance on the real dataset. This metric returns the F1 test score.

Generally, we interpret the “KS” and “CS” metrics to capture how well a model is able to replicate low-order marginals and the “DET” and “ML” metrics to capture the model’s ability to capture higher-order, more complex correlations. We follow this rough intuition in our later analysis.

4.2 Compute

Our experiments were conducted on a DGX box with 8 NVIDIA Tesla V100 GPUs, with each individual model run executed on a single GPU. Each model required roughly 20 minutes to 3 hours to train, depending on the input dataset size. This resulted in a total compute usage of approximately 200 GPU hours for our main experiments.

4.3 Benchmark

As shown in Table 2, we substantially outperform all three deep learning baselines included in our study, reaching performance comparable with the leading marginal-based approach, AIM (McKenna et al., 2022).

We use unbounded DP (following (Li et al., 2021; McKenna et al., 2022)) for all approaches, with a choice of $\epsilon = 1$ and $\delta = 1e - 9$ for all datasets and approaches.

4.4 Limitations of Marginal-based Approaches

Though AIM outperforms all other methods on our benchmark (see Table 2), a key limitation is that since it measures only low-order marginals, it cannot access the complex higher-order correlations

Method	KS \uparrow	CS \uparrow	DET \uparrow	ML (CLF) \uparrow	ML (REG) \uparrow
AIM	0.886 \pm 0.001	0.997 \pm 0.001	0.260 \pm 0.002	0.594 \pm 0.002	0.132 \pm 0.057
DP-TBART	0.847 \pm 0.001	0.978 \pm 0.002	0.172 \pm 0.004	0.554 \pm 0.005	-0.264 \pm 0.022
DPCTGAN	0.591 \pm 0.006	0.831 \pm 0.01	0.031 \pm 0.001	0.412 \pm 0.012	-2.83e4 \pm 2.31e4
DP-MERF	0.505 \pm 0.006	0.532 \pm 0.003	0.0 \pm 0.0	0.491 \pm 0.014	-4.2e20 \pm 2.5e20
DP-HFlow*	0.676 \pm 0.004	0.622 \pm 0.008	0.034 \pm 0.004	0.543 \pm 0.019	-0.603 \pm 0.345
DP-NTK	0.349 \pm 0.001	0.438 \pm 0.006	0.0 \pm 0.0	0.502 \pm 0.011	-5.83e16 \pm 4.76e16

Table 2: We evaluate AIM, DP-TBART, and four deep learning baselines against a variety of metrics, and report the average scores (and their standard errors) across all datasets. Note that ML (REG) may take on negative values if the regressor’s predictions perform worse on the real test data than a baseline that knows only the true mean. (*) For DP-HFlow, we re-implement this method as no code is publicly available.

that deep learning-based methods can. In this section, we will first propose a theoretical framework that precisely characterizes this limitation and then use this framework to find two real-world settings where marginal-based approaches fail to achieve good performance.

4.4.1 Theoretical Framework

We provide a theoretical analysis of marginal-based methods, which currently perform well on standard benchmarks, but are limited by construction in their ability to encode joint distributions with multiple interactions between variables. Our information theoretical framework demonstrates this limitation and gives a closed-form expression for the model’s divergence in the ideal setting of infinite data and privacy budget.

Preliminaries To begin, assume a data-generating process yields a discrete distribution $\bar{P}(X)$ defined on a sample space $\mathcal{X} = (V_1, \dots, V_K)$ with V_i disjoint w.r.t. each other as defined in Section 3.2. We refer to $\bar{P}(X)$ as the *true distribution*.

Next, a two-player adversarial game containing two agents, modeler and nature, ensues. The modeler is given access to the set of all marginals of order M , i.e., $\bar{P}(X_{i_1}, \dots, X_{i_M})$ for all possible subsets $\{i_1, \dots, i_M\} \subseteq \{1, 2, \dots, K\}$, but nothing else. This is consistent with a setting in which there is infinite data and an infinite privacy budget.

The modeler must propose a distribution $Q_M(X_1, X_2, \dots, X_K)$ such that all marginals match, i.e., $Q_M(X_{i_1}, \dots, X_{i_M}) = \bar{P}(X_{i_1}, \dots, X_{i_M})$ for all subsets $\{i_1, \dots, i_M\}$. We call the set of all distributions such that all marginals match Π_M . Then, nature reacts to Q_M and chooses $P_M \in \Pi_M$.

The modeler is asked to minimize the log loss $L(P_M, Q_M) = \mathbb{E}_{P_M}[-\log Q_M(x)]$, and nature maximizes the same quantity. We further assume that when nature encounters ties along level sets of $f(P_M) = L(P_M, Q_M)$, they are broken by deferring to maximizing the quantity $KL(Q_M || P_M)$ (but that any choice based on a further tie is arbitrary).

Results We first appeal to a set of results from Grünwald and Dawid (2004), which we restate as a single lemma using our notation.

Lemma 4.1. (*Grünwald and Dawid, 2004*)

1. *The modeler’s optimal estimate is uniquely given by the maximum entropy distribution $Q_M^* = \arg \sup_{P \in \Pi_M} H(P)$, where H is Shannon entropy.*
2. *$L(P, Q_M^*) = L(P', Q_M^*) = H(Q_M^*)$ for all $P, P' \in \Pi_M$.*

These initial results provide a couple of key insights. First, if a modeler acts optimally (in the sense that they pick the Q_M that, under an adversarial response from nature, achieves the lowest log loss), they will choose the maximum entropy distribution out of all of their available options: this in fact mirrors the behavior of current state-of-the-art marginal-based methods (McKenna et al., 2019; 2022). Second, given an optimal modeler, the log loss is the same no matter what distribution nature chooses, and in fact the log loss is equal to the entropy of the modeler’s guess. This second insight will prove useful in the proof for our central result, which we now state.

Theorem 4.2. $KL(Q_M^*||P) = H(Q_M^*) - H(P)$ for any $P \in \Pi_M$.

Proof. By Lemma 4.1, we know that $L(P, Q_M^*) = H(Q_M^*)$. The KL divergence is thus

$$KL(Q_M^*||P) = L(P, Q_M^*) - H(P) = H(Q_M^*) - H(P),$$

proving the theorem. □

Theorem 4.2 gives a closed-form expression for the KL divergence between the modeler’s estimated distribution and a hypothetical real distribution, expressed in terms of the entropy of the estimated distribution and the entropy of the real distribution. Theorem 4.2 thus highlights when we should expect the estimate from a marginal-based method to be good or bad: is the real distribution high-entropy or low-entropy? If the real distribution is high-entropy, then we should expect a marginal-based approach to achieve low KL divergence; on the other hand, if the real distribution is low-entropy, we should expect a marginal-based approach to provide a guess that is too “smoothed out”, and far away from ground truth. Furthermore, it grounds the intuition that the less information that is provided to the model (M is small), the larger the KL divergence. If less information is provided, then $H(Q_M^*)$ will be larger, and thus the KL divergence will also be larger. We continue discussion of Theorem 4.2 in Sections 4.4.2 and 4.4.3.

With Theorem 4.2 in hand, we can now quickly derive an impossibility result that makes the key limitation of marginal-based approaches precise.

Corollary 4.3. *When $M < K$, $KL(Q_M^*||P_M) > 0$.*

Proof. When a marginal-based method is not given the full joint $\hat{P}(X_1, \dots, X_K)$, then $|\Pi_M| \geq 2$. Since there is only one maximum entropy distribution Q_M^* (Lemma 4.1), and since nature breaks ties by choosing the distribution with the smallest entropy (Section 4.4.1 and Lemma 4.1), then that means $H(Q_M^*) > H(P_M)$, which implies that $KL(Q_M^*||P_M) > 0$. □

Since marginal-based approaches learn distributions via incomplete information (i.e., low-order marginals), then even in the most ideal of settings (infinite data, privacy budget), they cannot distinguish between one of potentially many choices of the true distribution: this leads to an error that does not asymptotically vanish with more data or privacy budget.

In the next two sub-sections, we present two empirical settings that demonstrate this exact limitation of marginal-based approaches.

4.4.2 Selected Datasets

In this section, we present two datasets with complex joint interactions—*Dyck-k* and WikiText-103 (Merity et al., 2016)—in which DP-TBART is able to achieve better performance than AIM under tight privacy guarantees. Both selected datasets are ideal testbeds for our approach because they serve as *worst-case* scenarios for the marginal-based approach. Seen through the lens of Theorem 4.2, measuring only low-order marginals leads to an estimated distribution with significantly higher entropy than the ground truth distribution (which contains much redundancy): this leads to a large KL divergence. Intuitively speaking, it is difficult for the marginal-based method to guess the higher-order correlations accurately, so we would expect its performance to be quite far from optimal.

Dyck Dataset In this section, we compare DP-TBART to AIM on *Dyck-k*, a family of datasets we define and artificially construct.⁴ Informally speaking, *Dyck-k* consists of all length k strings that belong to the Dyck formal language: the set of all strings with well-matched parentheses. Formally, we can define *Dyck* as the set of all strings generated by the following context-free grammar:

$$\begin{aligned} X \mapsto & (X) X \\ & | \epsilon, \end{aligned}$$

⁴Note that in NLP, *Dyck-k* may refer to the language of nested brackets of k types. We consider only languages with one bracket type.

Method	% Valid \uparrow
AIM	0.517
DP-TBART	0.804

Table 3: We evaluate DP-TBART against AIM on *Dyck-20* and report its performance with validity as the metric.

Method	GPT-2 Perplexity \downarrow
AIM	3948
DP-TBART	2945
DP-TBART (no privacy)	2334

Table 4: We compare perplexities of outputs from DP-TBART with outputs from AIM on the WikiText-103 dataset as evaluated by GPT-2.

where ϵ is the empty string.

Dyck-k is thus the set of all strings in *Dyck* with length k . To give a concrete example, “((()))” and “(())” belong to *Dyck-6*. On the other hand, “()()()” does *not* belong to *Dyck-6*; it has length 6 but does not have well-matched parentheses.

To study the performance of our approach, we construct a comprehensive dataset consisting of all strings in *Dyck-20*. Then, we evaluate each method by fitting it to the real dataset in a differentially private manner ($\epsilon = 1$ and $\delta = 1e - 9$), sample from the fitted model, and measure its performance by counting the frequency with which it samples syntactically correct strings.

In Table 3, we show the performance of our approach along with AIM. We find that our approach outperforms the competing marginal-based approach by a wide margin, achieving 80.4% accuracy in sampling syntactically correct strings.

While *Dyck-k* is an artificially-constructed dataset, it serves as a concrete empirical example of the limitations of marginal-based methods: even in the best of circumstances, they may be unable to capture the full complexity of a given joint distribution.

WikiText-103 We also compare DP-TBART to AIM on WikiText-103 (Merity et al., 2016), a real-world text dataset of Wikipedia articles. We split WikiText-103 into contiguous 50-character substrings and treat each substring as a row in our tabular dataset, where each column represents a distinct character index.

We evaluate each model by fitting to the processed dataset, sampling, and then taking the average of the perplexity of the sampled rows computed with GPT-2 (Radford et al., 2019). In Table 4, we show the performance of our approach, along with AIM. We find that our approach substantially outperforms AIM, achieving 25% lower perplexity, which suggests that the full joint distribution of characters is better captured by our approach than by AIM.

4.4.3 Low Privacy Setting

As pointed out in Corollary 4.3, even under the most generous assumptions (i.e., perfect marginal measurements, infinite data), marginal-based methods can fail to accurately capture the target distribution. On the other hand, deep learning-based methods have no such intrinsic limitation. In this section, we analyze what happens in practice when we approach this ideal noiseless setting by letting the privacy budget grow to $\epsilon = 100$ or greater.

In Figure 1, we show the performance of our approach and the leading marginal-based approach (McKenna et al., 2022) when varying ϵ on the Adult dataset. We find that while both approaches benefit from the increased privacy budget, our approach consistently outperforms the marginal-based approach across values of ϵ exceeding 1000 on the DET metric, suggesting that our approach is able to better capture higher-order correlations in the data when the privacy budget is relaxed.

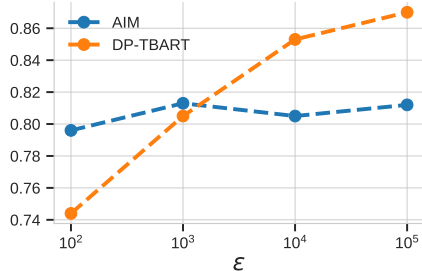


Figure 1: We show the performance (DET metric) of DP-TBART and AIM when varying ϵ on the Adult dataset.

5 Discussion

5.1 Deep Learning for Synthetic Data

Though synthetic data has been studied in the deep learning community, many studies overlook privacy concerns by failing to implement differential privacy, leading to potential leakage of private data (Xu et al., 2019; Zhao et al., 2021; 2022; Borisov et al., 2022; Kotelnikov et al., 2022). Additionally, these studies have also often neglected to compare their methods with state-of-the-art approaches (i.e., marginal-based).

In contrast, our work is the first to evaluate a deep learning method against the state-of-the-art across several datasets under strict privacy guarantees. We contextualize our results with further analysis, providing the first theoretical and empirical insights into the relative strengths of marginal-based methods and deep learning-based methods for synthetic tabular data generation.

5.2 The promise of deep learning-based approaches

Though DP-TBART does not outperform AIM on standard benchmarks, our auxiliary results suggest that deep learning-based methods can fill an important niche that marginal-based methods are not able to. We are optimistic that, through further investigation, deep learning-based approaches have the potential to surpass marginal-based methods in a broader range of scenarios or even pave the way for a hybrid method that incorporates the strengths of both approaches.

6 Conclusion

In this paper, we have presented an approach for differentially private synthetic tabular data generation based on deep learning. We have shown that, in certain settings, our deep learning-based approach is able to outperform state-of-the-art marginal-based approaches. We further provide a theoretical framework that formalizes the limitations of marginal-based methods and two empirical settings that demonstrate these limitations in action. Finally, we discuss the potential of deep learning-based approaches for further exploration.

We believe that our work serves as a promising starting point for understanding the utility of deep learning-based approaches for generating synthetic data under privacy guarantees, and hope that our results may inspire further exploration in this area.

6.1 Limitations & Broader Impact

Though our theoretical framework allows us to understand the limitations of different modeling strategies, it also rests on assumptions that are not satisfied in practice, e.g., infinite data and noiseless marginal measurements. Despite these unrealistic assumptions, we believe that the framework is intuitive enough to provide insight into practical settings (and confirm this with experiments, see Section 4.4.3). As for DP-TBART itself, it currently handles only discrete (or discretized) data, underperforms relative to the state-of-the-art marginal-based method, and requires GPU hardware to run efficiently. Despite row-level differential privacy guarantees, outputs from DP-TBART could still reflect underlying biases in the training data, which could lead to harm.

References

- M. Abadi, A. Chu, I. Goodfellow, H. B. McMahan, I. Mironov, K. Talwar, and L. Zhang. Deep learning with differential privacy. In *Proceedings of the 2016 ACM SIGSAC conference on computer and communications security*, pages 308–318, 2016.
- G. Arakelyan, G. Soghomonyan, and The Aim team. Aim, 6 2020. URL <https://github.com/aimhubio/aim>.
- V. Borisov, K. Seßler, T. Leemann, M. Pawelczyk, and G. Kasneci. Language models are realistic tabular data generators. *arXiv preprint arXiv:2210.06280*, 2022.
- C. M. Bowen and J. Snoke. Comparative study of differentially private synthetic data algorithms from the nist pscr differential privacy synthetic data challenge. *arXiv preprint arXiv:1911.12704*, 2019.
- L. Canale, N. Grislain, G. Lothe, and J. Leduc. Generative modeling of complex data. *arXiv preprint arXiv:2202.02145*, 2022.
- S. De, L. Berrada, J. Hayes, S. L. Smith, and B. Balle. Unlocking high-accuracy differentially private image classification through scale. *arXiv preprint arXiv:2204.13650*, 2022.
- D. Dua and C. Graff. UCI machine learning repository, 2017. URL <http://archive.ics.uci.edu/ml>.
- C. Dwork, F. McSherry, K. Nissim, and A. Smith. Calibrating noise to sensitivity in private data analysis. In *Theory of cryptography conference*, pages 265–284. Springer, 2006.
- W. Falcon and The PyTorch Lightning team. PyTorch Lightning, 3 2019. URL <https://github.com/Lightning-AI/lightning>.
- P. D. Grünwald and A. P. Dawid. Game theory, maximum entropy, minimum discrepancy and robust bayesian decision theory. *Annals of Statistics*, 2004.
- F. Harder, K. Adamczewski, and M. Park. Dp-merf: Differentially private mean embeddings with random features for practical privacy-preserving data generation. In *International conference on artificial intelligence and statistics*, pages 1819–1827. PMLR, 2021.
- A. Kotelnikov, D. Baranchuk, I. Rubachev, and A. Babenko. Tabddpm: Modelling tabular data with diffusion models. *arXiv preprint arXiv:2209.15421*, 2022.
- A. Kurakin, S. Chien, S. Song, R. Geambasu, A. Terzis, and A. Thakurta. Toward training at imagenet scale with differential privacy. *arXiv preprint arXiv:2201.12328*, 2022.
- J. Lee, M. Kim, Y. Jeong, and Y. Ro. Differentially private normalizing flows for synthetic tabular data generation. 2022.
- X. Li, F. Tramer, P. Liang, and T. Hashimoto. Large language models can be strong differentially private learners. *arXiv preprint arXiv:2110.05679*, 2021.
- T. Liu, G. Vietri, and S. Z. Wu. Iterative methods for private synthetic data: Unifying framework and new methods. *Advances in Neural Information Processing Systems*, 34:690–702, 2021.
- R. McKenna, D. Sheldon, and G. Miklau. Graphical-model based estimation and inference for differential privacy. In *International Conference on Machine Learning*, pages 4435–4444. PMLR, 2019.
- R. McKenna, B. Mullins, D. Sheldon, and G. Miklau. Aim: An adaptive and iterative mechanism for differentially private synthetic data. *arXiv preprint arXiv:2201.12677*, 2022.
- S. Merity, C. Xiong, J. Bradbury, and R. Socher. Pointer sentinel mixture models, 2016.
- S. Moro, P. Cortez, and P. Rita. A data-driven approach to predict the success of bank telemarketing. *Decision Support Systems*, 62:22–31, 2014.

- N. Papernot, M. Abadi, U. Erlingsson, I. Goodfellow, and K. Talwar. Semi-supervised knowledge transfer for deep learning from private training data. *arXiv preprint arXiv:1610.05755*, 2016.
- N. Papernot, S. Chien, S. Song, A. Thakurta, and U. Erlingsson. Making the shoe fit: Architectures, initializations, and tuning for learning with privacy. 2019.
- A. Paszke, S. Gross, F. Massa, A. Lerer, J. Bradbury, G. Chanan, T. Killeen, Z. Lin, N. Gimelshein, L. Antiga, A. Desmaison, A. Kopf, E. Yang, Z. DeVito, M. Raison, A. Tejani, S. Chilamkurthy, B. Steiner, L. Fang, J. Bai, and S. Chintala. PyTorch: An Imperative Style, High-Performance Deep Learning Library. In H. Wallach, H. Larochelle, A. Beygelzimer, F. d’Alché Buc, E. Fox, and R. Garnett, editors, *Advances in Neural Information Processing Systems 32*, pages 8024–8035. Curran Associates, Inc., 2019. URL <http://papers.neurips.cc/paper/9015-pytorch-an-imperative-style-high-performance-deep-learning-library.pdf>.
- N. Patki, R. Wedge, and K. Veeramachaneni. The synthetic data vault. In *2016 IEEE International Conference on Data Science and Advanced Analytics (DSAA)*, pages 399–410, Oct 2016. doi: 10.1109/DSAA.2016.49.
- A. Radford, J. Wu, R. Child, D. Luan, D. Amodei, I. Sutskever, et al. Language models are unsupervised multitask learners. *OpenAI blog*, 1(8):9, 2019.
- L. Rosenblatt, X. Liu, S. Pouyanfar, E. de Leon, A. Desai, and J. Allen. Differentially private synthetic data: Applied evaluations and enhancements. *arXiv preprint arXiv:2011.05537*, 2020.
- V. Sanh, L. Debut, J. Chaumond, and T. Wolf. Distilbert, a distilled version of bert: smaller, faster, cheaper and lighter. In *NeurIPS EMC2 Workshop*, 2019.
- Y. Tao, R. McKenna, M. Hay, A. Machanavajjhala, and G. Miklau. Benchmarking differentially private synthetic data generation algorithms. *arXiv preprint arXiv:2112.09238*, 2021.
- F. Tramer and D. Boneh. Differentially private learning needs better features (or much more data). *arXiv preprint arXiv:2011.11660*, 2020.
- A. Vaswani, N. Shazeer, N. Parmar, J. Uszkoreit, L. Jones, A. N. Gomez, Ł. Kaiser, and I. Polosukhin. Attention is all you need. *Advances in neural information processing systems*, 30, 2017.
- T. Wolf, L. Debut, V. Sanh, J. Chaumond, C. Delangue, A. Moi, P. Cistac, C. Ma, Y. Jernite, J. Plu, C. Xu, T. Le Scao, S. Gugger, M. Drame, Q. Lhoest, and A. M. Rush. Transformers: State-of-the-Art Natural Language Processing. pages 38–45. Association for Computational Linguistics, 10 2020. URL <https://www.aclweb.org/anthology/2020.emnlp-demos.6>.
- L. Xu, M. Skoularidou, A. Cuesta-Infante, and K. Veeramachaneni. Modeling tabular data using conditional gan. *Advances in Neural Information Processing Systems*, 32, 2019.
- Y. Yang, K. Adamczewski, D. J. Sutherland, X. Li, and M. Park. Differentially private neural tangent kernels for privacy-preserving data generation. *arXiv preprint arXiv:2303.01687*, 2023.
- J. Zhang, G. Cormode, C. M. Procopiuc, D. Srivastava, and X. Xiao. Privbayes: Private data release via bayesian networks. *ACM Transactions on Database Systems (TODS)*, 42(4):1–41, 2017.
- Z. Zhao, A. Kunar, R. Birke, and L. Y. Chen. Ctab-gan: Effective table data synthesizing. In *Asian Conference on Machine Learning*, pages 97–112. PMLR, 2021.
- Z. Zhao, A. Kunar, R. Birke, and L. Y. Chen. Ctab-gan+: Enhancing tabular data synthesis. *arXiv preprint arXiv:2204.00401*, 2022.

A Additional possible baselines

Despite the existence of CTAB-GAN+ (Zhao et al., 2022), a more recent deep learning approach that claims differential privacy guarantees, we did not evaluate against this model.

The original paper does not contain a complete proof that it satisfies differential privacy, and in fact there is reason to believe that it does not. The pre-processing pipeline is deterministic, even for continuous and mixed-type columns, for which it learns a Gaussian mixture. Furthermore, the privacy budget calculation remains the same even when both CTAB-GAN+ performs a modified batch sampling scheme that upweights infrequent rows (training-by-sampling) *and* takes gradient steps w.r.t. information loss, which is a deterministic function of real samples.

Note that while our paper does not contain an explicit proof of privacy, we have introduced no new mechanisms (such as training-by-sampling or modified batch sampling above), and thus the proof in Abadi et al. (2016) remains valid for our algorithm.

B Dataset sources and provenance

For ease of reproducibility and building off of our work, we will describe the provenance for our datasets: where they came from and what pre-processing steps we performed (if any).

B.1 Adult

- Link: <https://github.com/ryan112358/private-pgm/blob/master/data/adult.csv>
- Provenance: We downloaded the above CSV file without any further pre-processing.
- Description: This dataset is originally sourced from the UCI Machine Learning repository (Dua and Graff, 2017), but has been discretized in the process. The dataset contains personal attributes of U.S. residents, sampled in a stratified manner. The data was extracted from the 1994 U.S. Census.
- Licensing: Apache License 2.0

B.2 King

- Link: https://github.com/Team-TUD/CTAB-GAN-Plus/blob/main/Real_Datasets/king.csv
- Provenance: We downloaded the above CSV file without any further pre-processing.
- Description: The King dataset was originally obtained from this Kaggle dataset and contains house attributes (sqft, # of bathrooms, etc.) labeled with their sale price between 2014 and 2015 for King County, Washington.
- Licensing: CC0: Public Domain

B.3 Insurance

- Link: <https://www.kaggle.com/datasets/mirichoi0218/insurance>
- Provenance: We downloaded ‘insurance.csv’ without any further pre-processing
- Description: The Insurance dataset contains personal attributes (age, etc.) and U.S. medical insurance costs.
- Licensing: Database Contents License

B.4 Loan

- Link: <https://www.kaggle.com/datasets/itsmesunil/bank-loan-modelling>
- Provenance: We downloaded ‘Bank_Personal_Loan_Modelling.xlsx’ and processed it into a CSV.
- Description: The Loan dataset contains personal attributes from bank customers and a label (whether they converted from a depositor to loan customer).
- Licensing: CC0: Public Domain

B.5 Credit

- Link: <https://www.kaggle.com/mlg-ulb/creditcardfraud>
- Provenance: We downloaded the ‘creditcard.csv’ with a Kaggle account with no additional pre-processing.
- Description: The Credit dataset contains 30 numerical attributes describing credit card transactions along with a label for whether they were fraudulent.
- Licensing: Database Contents License

B.6 Bank

- Link: <https://archive.ics.uci.edu/ml/datasets/Bank+Marketing>
- Provenance: We downloaded ‘bank-full.csv’ from the UCI Machine Learning repository (Dua and Graff, 2017) with no additional pre-processing.
- Description: The Bank dataset (Moro et al., 2014) is derived from marketing campaigns from a bank. It contains personal attributes about a client and whether the client has subscribed to a product (bank term deposit).
- Licensing: Creative Commons Attribution 4.0 International

B.7 Census

- Link: <https://archive.ics.uci.edu/ml/datasets/Census+Income>
- Provenance: We downloaded ‘census.tar.gz’ from the UCI Machine Learning repository (Dua and Graff, 2017) and extracted it. Then, we combined census-income.data and census-income.test by concatenating both files together.
- Description: The Census dataset contains demographic and employment-related personal attributes from the U.S. Census Bureau, where each row corresponds to a stratified sample from the U.S. population.
- Licensing: Creative Commons Attribution 4.0 International

B.8 Car

- Link: <https://archive.ics.uci.edu/ml/datasets/Car+Evaluation>
- Provenance: We downloaded ‘car.data’ from the UCI Machine Learning repository (Dua and Graff, 2017) and performed no further pre-processing.
- Description: The Car dataset has only categorical columns and each row describes attributes of a different car model.
- Licensing: Creative Commons Attribution 4.0 International

B.9 Mushroom

- Link: <https://archive.ics.uci.edu/ml/datasets/Mushroom>
- Provenance: We downloaded ‘agaricus-lepiota.data’ from the UCI Machine Learning repository (Dua and Graff, 2017) and performed no further pre-processing.
- Description: The Mushroom dataset contains descriptions of hypothetical samples corresponding to 23 species of mushrooms.
- Licensing: Creative Commons Attribution 4.0 International

B.10 Poker Hands

- Link: <https://archive.ics.uci.edu/ml/datasets/Poker+Hand>
- Provenance: We downloaded ‘poker-hand-training-true.data’ from the UCI Machine Learning repository (Dua and Graff, 2017) and performed no further pre-processing.
- Description: The Poker Hands dataset contains hands of five playing cards and their corresponding class (in Poker).
- Licensing: Creative Commons Attribution 4.0 International

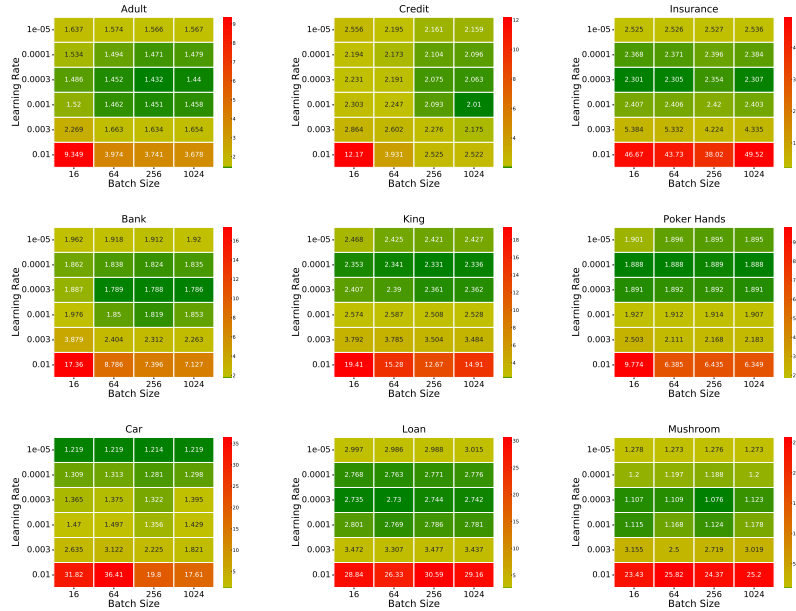


Figure 2: We train models with varying learning rates and batch sizes and evaluate the validation loss of each trained model.

C Hyperparameter Study

Given observations from past work from image and text domains that networks trained with differential privacy are sensitive to hyperparameters (Papernot et al., 2019; Li et al., 2021; De et al., 2022), we investigate whether the same phenomena occur in the tabular domain as well.

Learning Rate & Batch Size Our learning rate and batch size sweeps reveal behaviors that mirror those in networks trained on images (Kurakin et al., 2022; De et al., 2022) or text (Li et al., 2021): performance is highly sensitive to learning rate and batch size, and increasing batch size almost never hurts. See Figure 2 for a visualization of our results.

Clipping Norm We further study the behavior of the network under various clipping norms and precisely explain the underlying mechanism that causes the observed behavior. As shown in Figure 3, we find that the network behaves similarly to what has been empirically observed in images (Kurakin et al., 2022) and text (Li et al., 2021): decreasing the clipping norm until all gradients are clipped results in the best performance. Unlike prior work, however, we continue to evaluate the model at smaller and smaller values of C , and observe that the performance of the network actually stays constant and then begins to *rapidly degrade*.

While the plateauing in performance is explained by (1) the fact that Adam is gradient scale-invariant (i.e., scaling each gradient g by some scalar does not impact parameter updates) and (2) the fact that all gradients are clipped below $C = 1$, this does not adequately explain the rapid degradation of performance when C reaches 10^{-5} .

While it may be tempting to conclude that such significant degradation of performance is due to floating point imprecision, it turns out that the answer is much more subtle. Adam computes the effective step $\Delta_t = \alpha \cdot \hat{m}_t / (\sqrt{\hat{v}_t} + \epsilon)$ where $\epsilon = 1e - 8$ in practice and \hat{m}_t and $\sqrt{\hat{v}_t}$ are numerical estimates proportional to clipped gradient magnitude. When the gradient magnitudes reach the same order of magnitude as ϵ , the denominator of the fraction becomes dominated by ϵ and training begins to falter, as seen in Figure 3.

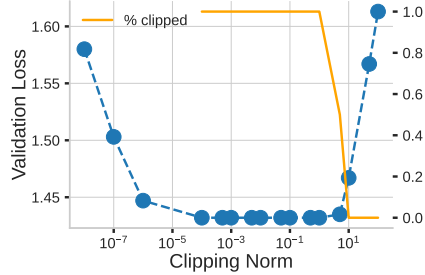


Figure 3: We show the impact of clipping norm on network performance on the Adult dataset.

D Software

For model implementation and training, we use Pytorch (Paszke et al., 2019) (BSD-3) and Lightning (Falcon and The PyTorch Lightning team, 2019) (Apache License 2.0). For experiment tracking, we use Aim (Arakelyan et al., 2020) (Apache License 2.0). For our transformer model, we adapted DistilGPT-2 (Sanh et al., 2019) from Hugging Face Transformers (Wolf et al., 2020) (Apache License 2.0).

For our DP-SGD implementation, we use private-transformers (Apache License 2.0).

E Poisson sampling

While some previous works sample batches non-privately by shuffling the training dataset and picking uniform batches (Li et al., 2021; Tramer and Boneh, 2020), we ensure end-to-end differential privacy guarantees by implementing Poisson sampling. Since the Binomial distribution $B(n, p)$ concentrates tightly around its mean when n is large and p is small, we observe that out-of-memory issues do not occur in practice, and micro-batching was not required.

F Column Ordering

One might observe that an autoregressive approach introduces an additional high-dimensional hyperparameter: column ordering. In our experiments, we attempted several strategies (ordering columns from ones with largest cardinalities to smallest, smallest to largest, and toposorting a graph learned via structure learning), but observed no consistent impact on performance.